Atmospheric Environment 126 (2016) 117–127

Contents lists available at ScienceDirect

Atmospheric Environment

journal homepage: www.elsevier.com/locate/atmosenv

Spatial and temporal variations of spring dust emissions in northern China over the last 30 years

Hongquan Song [a], Kesheng Zhang [a], Shilong Piao [b], Shiqiang Wan [a, *]

[a] College of Life Sciences, State Key Laboratory of Cotton Biology, Key Laboratory of Plant Stress Biology, Henan University, Kaifeng, Henan 475004, China
[b] Sino-French Institute for Earth System Science, College of Urban and Environmental Sciences, Peking University, Beijing 100871, China

HIGHLIGHTS

- Spatial pattern of dust flux in northern China over last 30 years was simulated.
- Temporal trend of dust emissions in northern China over last 30 years was simulated.
- Climate change and human activities significantly influence dust emissions in China.

ARTICLE INFO

Article history:
Received 18 June 2015
Received in revised form
16 November 2015
Accepted 23 November 2015
Available online 27 November 2015

Keywords:
Wind erosion
Integrated wind erosion modeling system
Spatial-temporal patterns
Human activities
Climate change

ABSTRACT

Dust emissions caused by wind erosion have significant impacts on land degradation, air quality, and climate change. Dust from the arid and semiarid regions of China is a main contributor to atmospheric dust aerosols in East Asia, and their impacts can stretch far beyond the territory of China. Spatial-temporal patterns of dust emissions in China over the last several decades, however, are still lacking, especially during the spring season. In this study, we simulated the spatial-temporal dynamics of spring dust emissions from 1982 to 2011 in arid and semi-arid areas of China using the Integrated Wind Erosion Modeling System. Results showed that the most severe dust emission events occurred in the Taklimakan Desert, Badain Jaran Desert, Tengger Desert, and Ulan Buh Desert. Over the last three decades, the magnitude of spring dust emissions generally decreased at the regional scale, with an annual spring dust emission of ~401.10 Tg. Among different vegetation types, the highest annual spring dust emission occurred in the desert steppes (~163.95 Tg), followed by the deserts (~103.26 Tg). The dust emission intensity in the desert steppes and the deserts was ~150.83 kg $km^{-2} \cdot yr^{-1}$ and ~205.46 kg $km^{-2} \cdot yr^{-1}$, respectively. The spatial patterns of the inter-decadal variation are related to climate change and human activities. Mitigation strategies such as returning farmland to grassland, fenced grazing, and adequate grass harvesting, must be taken to prevent further soil losses and grassland degradation in northern China.

1. Introduction

Wind erosion is a natural geological process that includes detachment, transport, and deposition of soil particles by strong winds (Li et al., 2007; Hoffmann et al., 2011). It is a major soil degradation process in arid and semi-arid areas of the world (Gregory et al., 2004; Buschiazzo and Zobeck, 2008; Webb et al., 2009). Global dust emissions are estimated to range from 1018 Tg yr^{-1} (Miller et al., 2004) to 3000 Tg yr^{-1} (Tegen and Fung, 1994), which accounts for approximately 30%–50% of the total aerosol injections into the atmosphere (Alfaro, 2008). Dust aerosols have significant impacts on the Earth's radiation budget, global biogeochemical cycles, terrestrial soil formation, atmospheric chemistry, air quality, and public health (Chadwick et al., 1999; Reynolds et al., 2001; Jickells et al., 2005; Li et al., 2007; Alfaro, 2008; Chappell et al., 2012). In addition, the detachment and transport of dust can significantly lower soil fertility and water holding capacity in dust source areas (Li et al., 2007). The deposition of dust may also have significant beneficial effects, however, such as the transport of organic carbon (Chappell et al., 2012, 2013), nitrogen (Mace et al., 2003), phosphate (Eger et al., 2013), iron

* Corresponding author. College of Life Sciences, Henan University Jinming Campus, Kaifeng, Henan Province, China.
E-mail address: swan@henu.edu.cn (S. Wan).

http://dx.doi.org/10.1016/j.atmosenv.2015.11.052
1352-2310/

(Conway et al., 2015; Horner et al., 2015), and other essential nutrients from the soil to terrestrial and aquatic ecosystems that can enhance primary productivity (Chadwick et al., 1999; Neff et al., 2008; Field et al., 2009).

In order to assess the impacts of dust emissions on socio-economics and the environment, it is essential to quantify the wind erosion rates at different spatial and temporal scales. Wind erosion is affected by complex interactions among soil properties, climate, vegetation, and land management (Lu and Shao, 2001; Hoffmann et al., 2011; Aubault et al., 2015). Several approaches have been taken to measure the physical properties and driving factors of wind erosion. For example, mathematical simulations are used to derive the relationships between meteorological records and interacting surface parameters (McTainsh et al., 1998). Remote sensing and geographic information systems (GIS) are applied to estimate the wind erosion intensity (Zobeck et al., 2000; Maman et al., 2011; Guo et al., 2013), while further identifying dust sources (Ginoux et al., 2004). A large number of wind erosion models have been developed to quantify wind erosion rates, soil losses, and dust emissions at the local (Fryrear et al., 1998, 2001; Okin, 2008), regional (Lu and Shao, 2001), and global scales (Webb et al., 2009).

In northern China, wind erosion is a serious environmental problem, especially in arid and semi-arid regions (Chen et al., 2014) that experience heavy and long-term grazing. The average annual soil dust emission in East Asia is ~214 Tg (Tanaka and Chiba, 2006), and 32% of these emissions occur in northern China (Tanaka and Chiba, 2006). To identify dust sources and sinks in China, a wind erosion risk map with high spatial resolution has been developed based on remote sensing images (Reiche et al., 2012). With the integration of remote sensing, experiments, and field observations, Liu and Wang (2014) have explored aeolian processes and landscape changes of the Sonid grassland in northern China. Using meteorological (Sun et al., 2001) and remote sensing data (Taramelli et al., 2012; Gong et al., 2014), spatial-temporal variations of dust storms and wind erosion intensity have been examined over the last several decades in northern China.

Few studies have investigated spatial and temporal variations of dust storms or land desertification (Sun et al., 2001; Wang et al., 2004), however, spatial patterns and temporal trends of the quantity of soil losses due to wind erosion over the last several decades in northern China remain limited. To improve on this limitation, in this study, we simulate the spatial-temporal variations of spring dust emissions during the period 1982–2011, using the Integrated Wind erosion Modeling System (IWEMS; Lu and Shao, 2001). Moreover, direct links between regional climate change and dust emissions have not yet been made. Thus our study will also attempt to discuss the interconnections that exist between dust emissions and climate change in northern China over the last three decades.

2. Materials and methods

2.1. Study area

This study area is located in hyper arid, arid, and semiarid regions in northern China (Fig. 1), which accounts for 30% of the total area of China, and is classified as a temperate continental climate, including vegetation types such as grasslands, shrublands, and deserts. The mean annual precipitation is generally less than 400 mm in research region.

2.2. Wind erosion model description

IWEMS is a process-based model developed by Lu and Shao (2001), and consists of an atmospheric model, a land surface scheme, a wind erosion scheme (for dust emission and sediment drift), a dust transport and deposition scheme, and a geographic information database (Shao et al., 2002). The atmospheric model provides relevant data (e.g. wind velocity and eddy diffusivity) used in driving both the wind erosion and dust transport model. In order to compute the dust emission rate, relevant atmospheric data and land surface data are passed to the wind erosion scheme at each physical time step. The GIS database provides the spatially distributed land surface data (e.g. soil properties, friction velocity) required for the wind erosion scheme. The dust emission data produced by the dust emission model are then passed to the dust transport model together with atmospheric data for the prediction of dust motion (Shao et al., 2003). The IWEMS has been extensively used to simulate dust over East Asia (Shao et al., 2002; Mao et al., 2011, 2013; Du et al., 2014).

2.3. Datasets

The land surface variables required by the IWEMS are soil properties, vegetation cover, and land use. Soil variables (e.g., soil types, soil bulk density) are obtained from the Harmonized World Soil Database (HWSD) with a map scale of 1:1,000,000. Land use maps with a map scale of 1:100,000 in 1980s, 1995, and 2000 are obtained from the Data Sharing Infrastructure of Earth System Science (http://www.geodata.cn/), which are integrated with soil data to extract the fraction of erodible area according to the methods in Lu and Shao (2001). The monthly vegetation cover is calculated from the normalized deviation vegetation index (NDVI) formula of Gutman and Ignatov (1998). The NDVI datasets for 1982–2011 are obtained from the Global Land Cover Facility, Global Inventory Modeling and Mapping Studies (Tucker et al., 2005), which have a spatial resolution of 8 km × 8 km. Wind field datasets are provided by the National Centers for Environmental Prediction and National Center for Atmospheric Research (NCEP/NCAR) reanalysis datasets, which are updated every six hours with a spatial resolution of 2.5° × 2.5°. To drive the IWEMS, these three datasets are projected to the same spatial coordinate system using the Albers map projection, and are also re-gridded to the same spatial resolution of 8 km × 8 km.

To validate the performance of the IWEMS, simulation output is compared to the daily spring dust storm frequency data observed at 283 meteorological stations during the period 1982–2007, which are obtained from the meteorological network of the China Meteorological Administration (Zhou et al., 2006). Dust comparison data are further used to explore the relationship between the dust storm frequency and the dust emissions. Daily wind velocity, precipitation, and temperature at 365 meteorological stations over the last 30 years in the research region are obtained from the China Meteorological Data Center (http://data.cma.gov.cn). Meteorological comparison data are further used to explore the impacts of inter-decadal change of wind velocity, precipitation, and temperature on dust emissions in northern China over the last three decades.

2.4. Model simulation and validation

This study uses the IWEMS to simulate the spatial patterns of dust flux and the quantity of dust emissions at a regional scale in the spring season of March 1 to May 31 during the period of 1982–2011. IWEMS is driven by atmospheric conditions that are updated every 6 h, vegetation cover that is updated annually, and land surface properties that are either updated on a decadal scale (e.g., land use), or held constant (e.g., soil properties) depending on the land surface variable. Soil moisture is not included because the arid and semi-arid areas studied in this work experience minimal

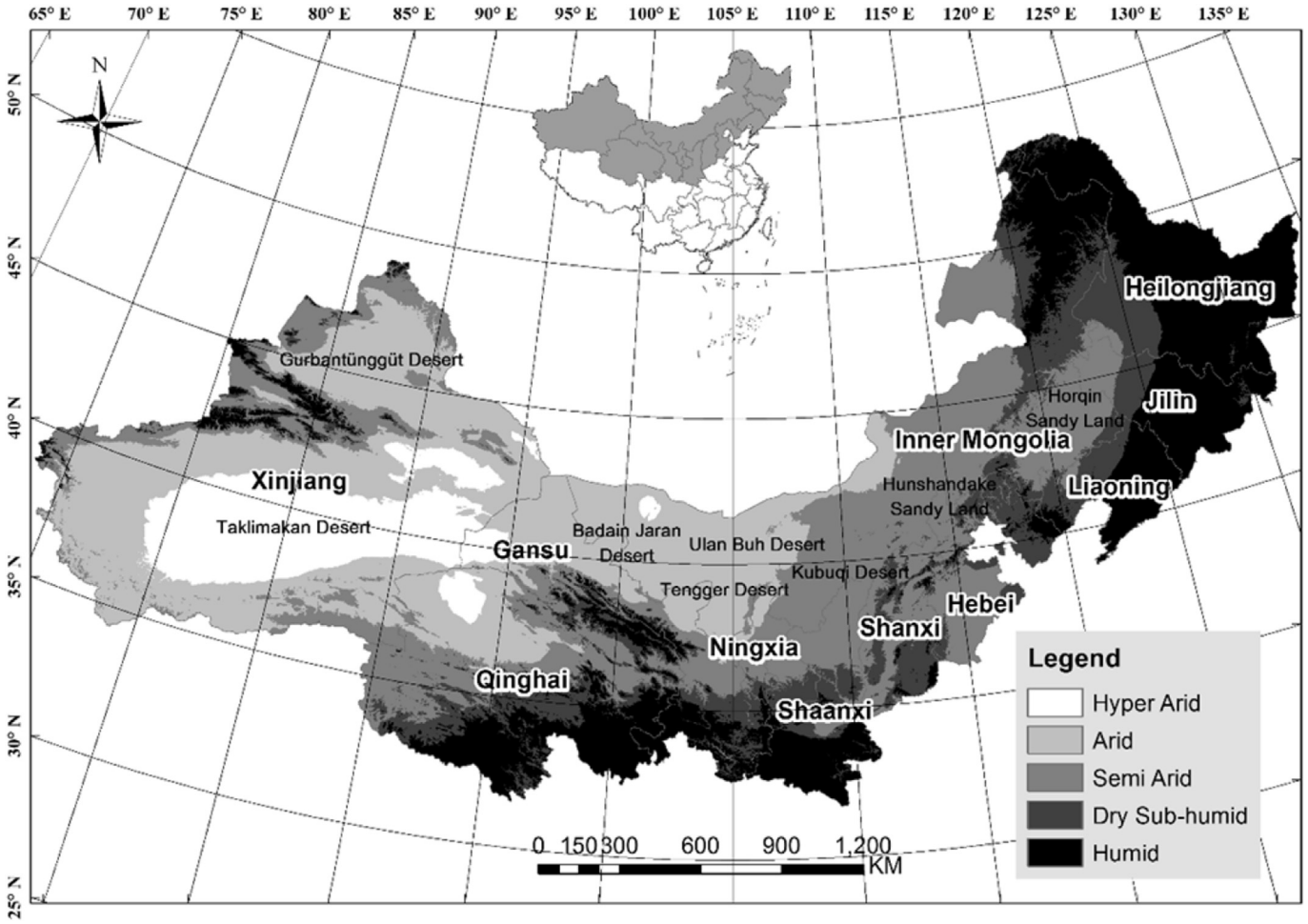

Fig. 1. Spatial distribution of arid intensity and deserts in northern China.

precipitation during the springtime. This simulation was restricted to the suspension of soil particles less than 90 μm, as these particle sizes are most readily emitted into the atmosphere from dust source regions.

Dust emission observations are scarce in northern China, which makes it challenging to provide a comprehensive evaluation of the IWEMS performance. Thus we first assume that dust emissions are correlated with dust storm frequency, while using previous studies (Shao and Leslie, 1997; Fécan et al., 1998) that show dust emissions are highly correlated with areas of high wind velocity and low precipitation. Under this premise, our dust model simulations may then be partially validated by correlative analysis between dust emissions, dust storm frequencies, and precipitation at meteorological stations in the research region.

3. Results

3.1. Spatial patterns of spring dust emissions

The spatial distribution of annual dust flux (Fig. 2a) showed that the most significant dust sources in northern China over the last three decades were found in the Taklimakan Desert, Badain Jaran Desert, Tengger Desert, Ulan Buh Desert, northwest Qinghai Province, and northwest Gansu Province (Figs. 1 and 2a). The spring dust flux was more than 200 $g \cdot m^{-2} \cdot yr^{-1}$ in most of these regions. Regions of enhanced wind erosion in China were in the hyper arid, arid, and semi-arid areas (Figs. 1 and 2a) covered by desert, desert-steppe, and gobi desert, where the vegetation cover was lower than 0.20 (Fig. 2b).

The dust flux was higher in April than in March in most regions, including central and western Inner Mongolia, northwestern Gansu, northwestern Qinghai, and eastern Xinjiang (Fig. 3a, b, d). In central Taklimakan Desert, southwestern Xinjiang, and some regions in Qinghai, however, the dust flux in April was in fact lower than in March (Fig. 3a, b, d). The dust flux in May was higher than in March in most areas of the research region (Fig. 3a, c, e), except in southwestern Xinjiang. The dust flux exhibited a seasonal decrease in most regions, except for southeastern Xinjiang and northwest Qinghai from April to May in northern China over the last 30 years (Fig. 3b, c, f).

Spatial distributions of inter-decadal dust flux differences were calculated by taking the annual average of spring dust fluxes during the1980s (1982–1989), 1990s (1990–1999), and 2000s (2000–2011) (Fig. 4). Fig. 4a, b, and d illustrated that the spring dust fluxes in Inner Mongolia, Gansu, and most of Qinghai were higher in the 1980s compared to the 1990s. Higher dust flux regions were concentrated in the Taklimakan Desert, parts of northern Xinjiang, and parts of northwestern Qinghai (Fig. 4a, b, d). The decadal dust flux in northwestern Inner Mongolia, eastern Xinjiang and Taklimakan Desert during the 1980s was lower compared to the 2000s (Fig. 4a, c, e). The decadal spring dust flux in 1990s was also lower compared to the 2000s across a most of the region (Fig. 3b, c, f),

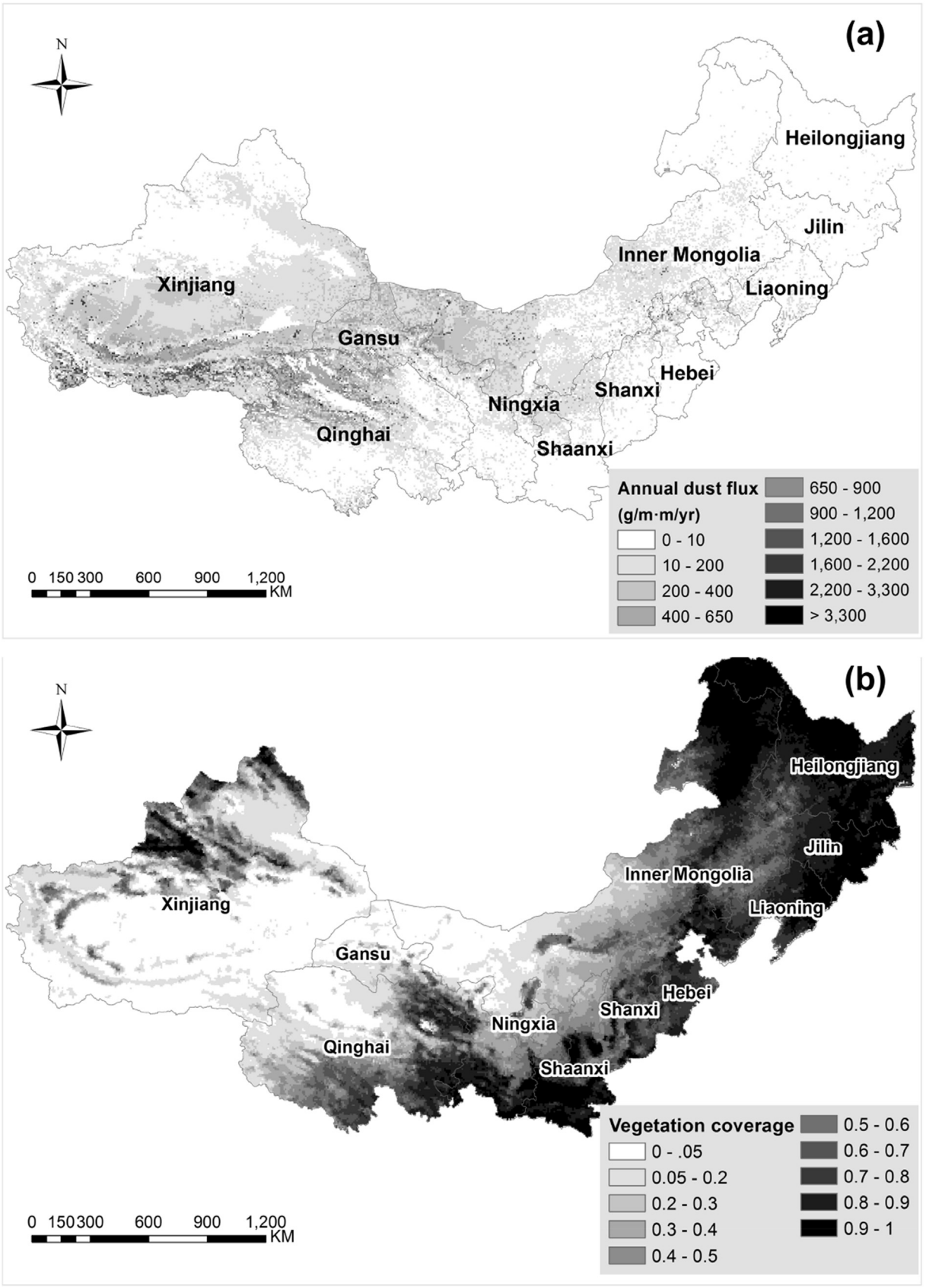

Fig. 2. Spatial distribution of annual spring dust flux (a) and the annual vegetation cover (b) in northern China over the last three decades.

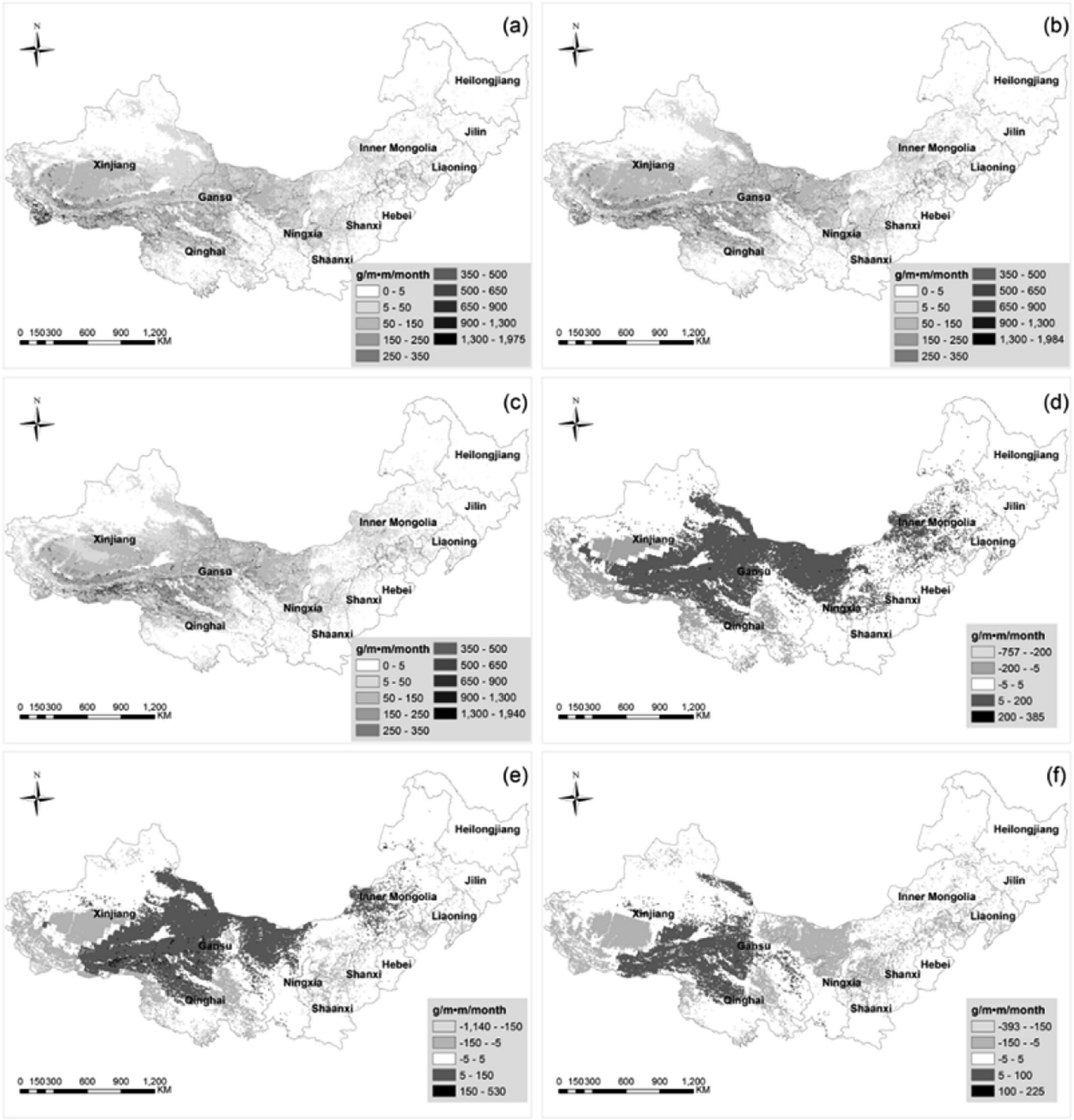

Fig. 3. Spatial distributions of the dust flux in March (a), April (b), May (c), and the spatial differences of April–March (d), May–March (e), and May–April (f) in northern China from 1982 to 2011.

except for in western and eastern Taklimakan Desert, parts of southern Xinjiang, and parts northern Shaanxi, where the dust fluxes were higher in the 1990s.

3.2. Temporal trends of dust emissions

The annual spring average dust emissions simulated in northern China generally declined between 1982 and 2005, however, dust emissions increased since 2005 (Fig. 5). The observed dust storm frequency exhibited a similar decreasing pattern from 1982 to 1997, and generally increased until 2007. The dust storm frequency was defined as the total number of dust storms observed at all the meteorological stations in the research region. The maximum, minimum, and average spring dust emissions for 1982–2011 were 463.33 Tg in 1996, 316.21 Tg in 2005, and 401.10 Tg, respectively. The monthly average dust emissions in March, April, and May were ~122.65 Tg, ~142.48 Tg, and ~135.97 Tg, respectively. A maximum in dust emissions for April was consistent with the spatial patterns of

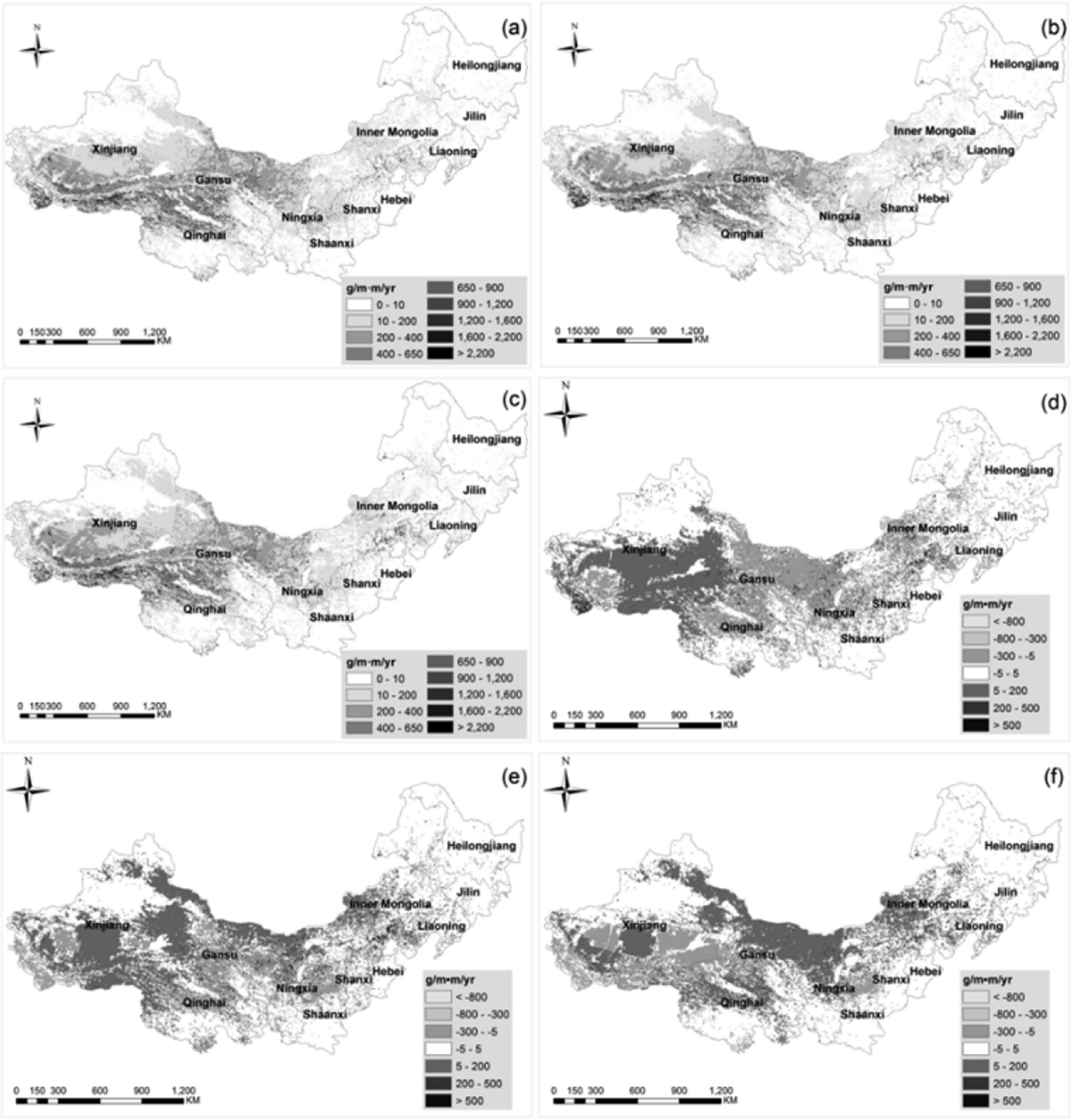

Fig. 4. Spatial distributions of the annual dust flux in the 1980s (a), 1990s (b), and 2000s (c), and the spatial differences of the 1990s−1980s (d), 2000s−1980s (e), and 2000s −1990s (f) in northern China.

monthly dust flux (Fig. 3).

Table 1 lists the different types of vegetation cover in the research region of northern China. The largest vegetation type in this region is desert steppes, with an area of 1.08×10^6 km^2. The trends in dust emissions for different vegetation types (Fig. 6) were calculated using the vegetation type dataset and the spatial distribution of annual average spring dust emissions from 1982 to 2011. The desert steppes had the largest dust emissions in northern China (Fig. 6a), followed by the deserts and the steppes. Dust emissions for other vegetation types were much lower than these three vegetation types. Dust emissions in the desert steppes and the steppes decreased slightly over the last three decades, however, the dust emissions in the deserts had a slight increasing trend. The dust emission intensities (Fig. 6b) were calculated for each vegetation type based on the amount of dust emissions divided by the vegetation type area. We found that the deserts had the largest dust emission intensity, followed by the desert steppes and the alpine vegetation (Fig. 6b).

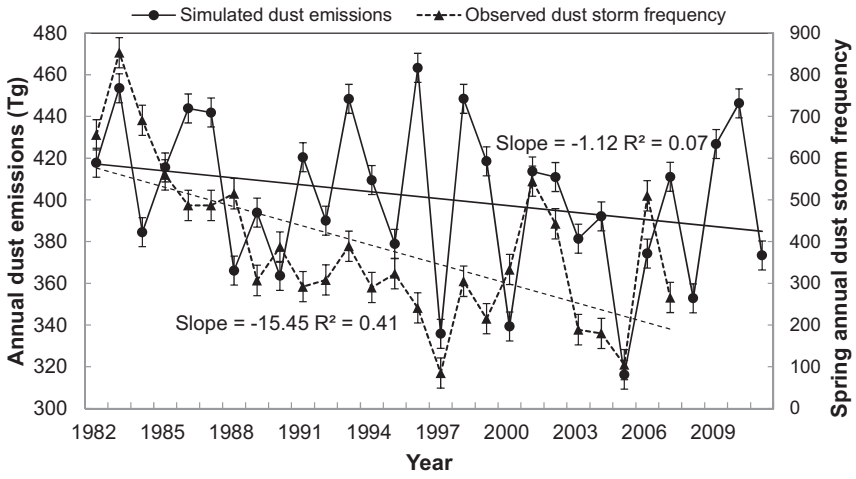

Fig. 5. Temporal trends in the annual average spring (March–May) for simulated dust emissions (1982–2011; solid line – primary y-axis), compared to the observed dust storm frequency (1982–2007; dashed line) in northern China.

Table 1
Areas of different vegetation types in the research region.

Vegetation type	Area (km^2)
Desert steppes	1.08×10^6
Steppes	8.45×10^5
Cultivated vegetation	8.12×10^5
Meadows	6.27×10^5
Deserts	5.02×10^5
Broadleaf forests	3.82×10^5
Shrubs	2.02×10^5
Needleleaf forests	1.86×10^5
Alpine vegetation	1.67×10^5
Grasslands	0.65×10^5
Marshes	0.52×10^5
Needleleaf and broadleaf mixed forests	0.15×10^5

3.3. Evaluation of simulated dust emissions

To evaluate the results from IWEMS, a comparison was made between simulated dust flux and observed dust storm frequencies at each meteorological station across the research region between 1982 and 2007. A linear least squares regression analysis was performed using the simulated annual dust flux at meteorological stations as the dependent variable, and the observed annual dust storm frequency as the independent variable. The simulated dust flux was positively correlated with observed dust storm frequencies (Fig. 7a). The square of the correlation coefficient, R^2, was high at 0.76 ($P < 0.005$). Furthermore, the tendency and fluctuations of annual (Fig. 5) total spring dust storm frequencies at all meteorological stations were in good agreement with simulated dust emissions from 1982 to 2007.

There was significantly less correlation between dust emissions and wind velocity (Fig. 7b), with a low R^2 value of 0.02 ($p < 0.01$). This poor correlation was due to the complex conditions of land surface. The dust flux declined nonlinearly with the increased precipitation (Fig. 7c). The spatial distribution of observed annual dust storm frequencies for spring (Fig. 8) agreed well with the simulated dust flux levels at each meteorological station.

4. Discussion

In this study, the annual average of simulated spring dust emission in northern China was 401.10 Tg during spring, which is much larger than the results in east Asia where the simulated dust emissions are 214 $Tg \cdot yr^{-1}$ (Tanaka and Chiba, 2006). This could have been ascribed to the different range in soil particle diameters used in the simulations. Our simulation focuses on soil particle diameters that are less than 90 μm, however, the dust emissions simulated in Tanaka and Chiba (2006) limited the diameter to between 0.2 μm and 24 μm. The dust emissions in 1996, 1998, 2001, and 2006 are much higher than their previous years 1995, 1997, 2000, and 2005 (Fig. 5), which could be caused by extreme droughts in 1995, 1997, 2000, and 2005 (Wang et al., 2003, 2011; Ma and Fu, 2006; Yu et al., 2014) in northern China. Furthermore, a severe drought event in northern China during the winter of 2008–2009 (Gao and Yang, 2009) caused the dust emissions to sharply increase from 352.86 Tg to 426.80 Tg in 2009, and then to 446.35 Tg in 2010 (Fig. 5). Extreme drought events can reduce the vegetation density and coverage (Zender and Kwon, 2005), while subsequently leading to higher dust emissions for the next few years. The dust emissions sharply decrease from 446.35 Tg to 373.40 Tg in 2011 (Fig. 5), which could be a result of the low temperature in the winter of 2010 and the spring of 2011 (Duan et al., 2013). Lower temperatures may delay the melting of the frozen ground, leading to decreased dust emissions.

Dust emissions are strongly under the influence of climate change (Lambert et al., 2008) and human activities (Sokolik and Toon, 1996; Mulitza et al., 2010). It is essential to improve our understanding of the impacts of climate change and human activities on the spatial and temporal variations of dust emissions over the last 30 years in northern China. The downward trend of the dust emission simulated by IWEMS is consistent with the trend of decreased dust storms (Qian et al., 2002; Wang, 2005), as well as increased visibility (Mahowald et al., 2007) during this period. This phenomenon could have been caused by the atmospheric warming and pressure reductions over northern Asia between 1982 and 2000 (Qian et al., 2002; Grigholm et al., 2015), which may potentially reduce temperature/pressure gradients and lead to lower zonal wind velocities (Li, 2015).

Dust sources are mainly concentrated in the areas of high wind velocity (Fig. 7b) and low precipitation (Fig. 7c). To investigate the impacts of climate change on dust emissions, we analyzed the inter-decadal difference of spring wind velocity (Fig. 9a), precipitation (Fig. 9b), and temperature (Fig. 9c) at all meteorological stations, compared to the dust flux change during the periods of 1980s–1990s, 1980s–2000s, and 1990s–2000s. Wind velocities

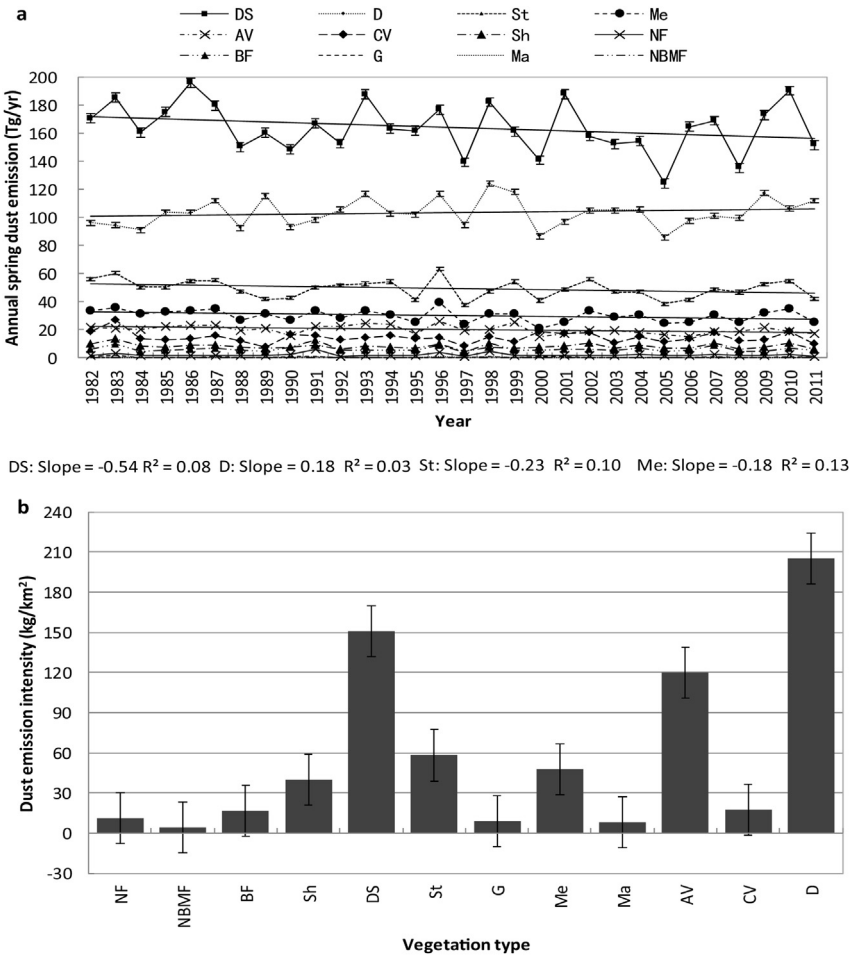

Fig. 6. Dust emission (a) trends and (b) intensities for different vegetation types from 1982 to 2011. The vegetation types are desert steppes (DS), deserts (D), steppes (St), meadows (Me), alpine vegetation (AV), cultivated vegetation (CV), shrublands (Sh), needleleaf forests (NF), broadleaf forests (BF), grasslands (G), marshes (Ma), needleleaf and broadleaf mixed forests (NBMF).

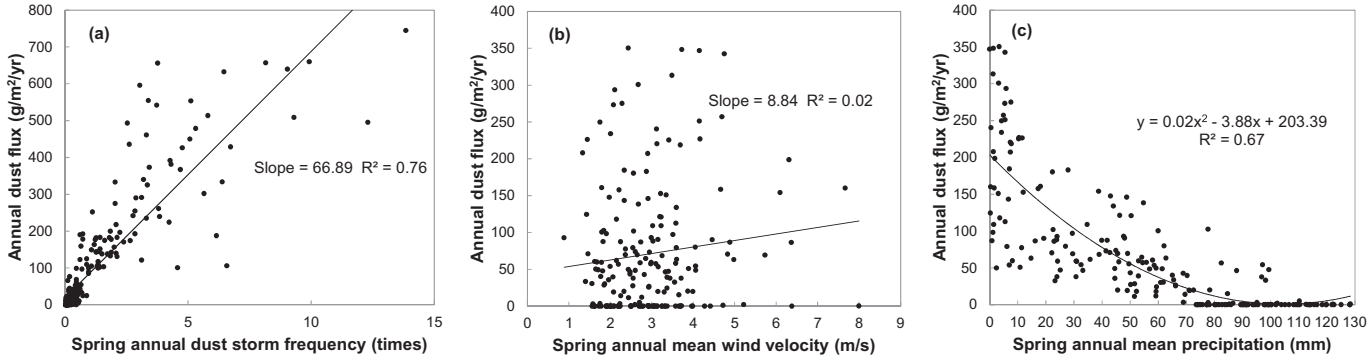

Fig. 7. X–Y scatter plots of the simulated annual dust flux compared to the observed (a) annual dust storm frequency, (b) mean wind velocity, and (c) mean precipitation for all meteorological stations in northern China during the spring season between 1982 and 2007.

and corresponding dust emissions generally decreased for both the 1980s–1990s and 1980s–2000s (Fig. 9a). During the period of 1990s–2000s (Fig. 9a), however, the wind velocity at numerous meteorological stations increased, which led to increased dust emissions at some stations. Precipitation is not the primary controlling factor on dust emissions in China (Fig. 9b), although it could partly inhibit the dust emission in some regions. At locations of increased temperature, dust emissions are also enhanced. Thus enhanced temperature may be a surrogate for more significant water stresses due to higher transpiration and evaporation from shallow soil depths (Munson et al., 2011), which would accelerate the likelihood of dust emissions from disturbed soil surfaces.

The vegetative land cover is a major factor affecting soil wind erosion processes and dust emissions (Engelstädter et al., 2003; Zender and Kwon, 2005; Kurosaki and Mikami, 2007). A shift to more grasslands land cover caused by climate change in the past 30

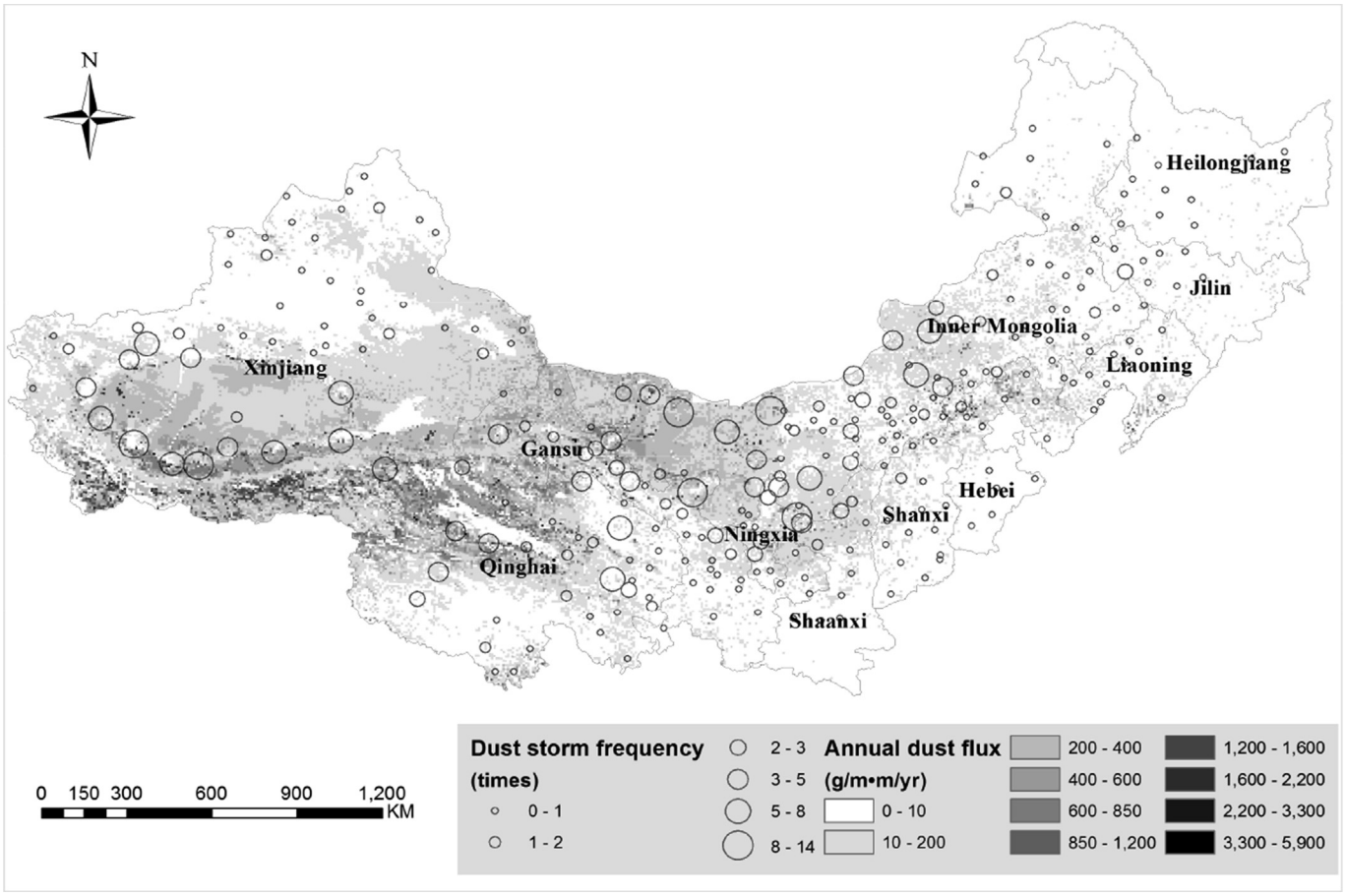

Fig. 8. Spatial overlay of observed dust storm frequency and the simulated annual dust flux in northern China for the spring periods between 1982 and 2007.

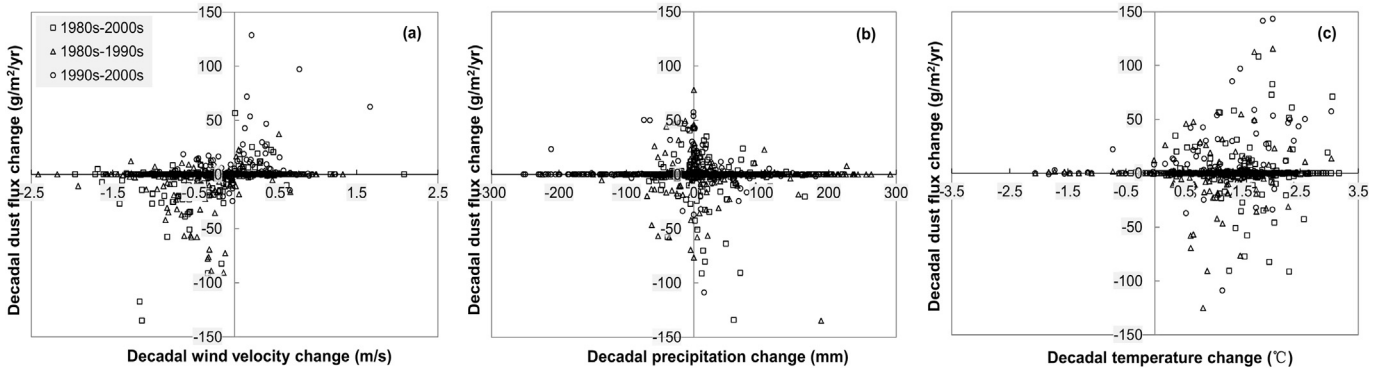

Fig. 9. Inter-decadal dust flux changes compared to the inter-decadal (a) wind velocity changes, (b) precipitation changes, and (c) temperature changes for the spring periods of 1980s–1990s (triangles), 1980s–2000s (squares), and 1990s–2000s (circles).

years in northern China (Piao et al., 2003, 2006; Li et al., 2014) leads to decreased dust emissions in the regions of steppe and desert steppe (Fig. 6a). Various human activities (Neff et al., 2008; Xu et al., 2014), such as land use practices, can significantly affect vegetation (Sokolik and Toon, 1996), which can result in additional dust emissions. The degraded land are due to desertification in northern China has been accelerated 3600 km^2 yr^{-1} from 1987 to 2000 (Wang et al., 2004; Wang, 2014), and the annual expansion rate from 2000 to 2010 is −1375 km^2 (Wang, 2014). This may be a driving factor for the increased dust emission in desert from 1982 to 1999 (Fig. 6a). The annual dust emission in the desert regions during the 2000s was 101.53 Tg, which is lower than the 107.11 Tg for the 1990s (Fig. 6a) suggesting that a retreat of the sandy deserted land may have contributed to the decreased dust emissions in desert regions from 2000 to 2011.

Considering dust source areas have low precipitation during the spring, we did not include the soil moisture parameter in our simulations. Moreover, the simulation results presented here suffer from additional uncertainties due to the coarse spatial resolution of 2.5° × 2.5°, thus largely simplifying the complexity of the wind field. Although the scarcity of dust flux observations in China is a limiting factor preventing a comprehensive evaluation in this

study, the results here provide useful spatial and temporal patterns of dust emissions for 1982–2011 in northern China.

5. Conclusions

This study has demonstrated that dust sources are mainly distributed in areas where the vegetative coverage is lower than 20% that spring dust emissions in the research region generally experience a decreasing trend for 1982–2011. Our observations suggest that climate change and human activities are significantly impacting dust emissions over northern China. Responses of dust emissions to climate change, however, are dependent on the regions investigated. Thus it is necessary to take measures to prevent overgrazing, grassland degradation, and soil loss in northern China, such as returning farmland to grassland, fenced grazing, inhibiting further grass cutting, and implementing scientific policy for stocking capacity.

Acknowledgments

We the authors thank Patrick Campbell and Shufei Song for help in improving the language, and also thank Dafeng Hui, Youmin Chen, and Pengfei Liu for providing valuable comments and technologies on this manuscript. This study was financially supported by the Ministry of Science and Technology of China (2013CB956300) and the National Natural Science Foundation of China (41401107).

Appendix A. Supplementary data

Supplementary data related to this article can be found at http://dx.doi.org/10.1016/j.atmosenv.2015.11.052.

References

Alfaro, S.C., 2008. Influence of soil texture on the binding energies of fine mineral dust particles potentially released by wind erosion. Geomorphology 93, 157–167.
Aubault, H., Webb, N.P., Strong, C.L., McTainsh, G.H., Leys, J.F., Scanlan, J.C., 2015. Grazing impacts on the susceptibility of rangelands to wind erosion: the effects of stocking rate, stocking strategy and land condition. Aeolian Res. 17, 89–99.
Buschiazzo, D.E., Zobeck, T.M., 2008. Validation of WEQ, RWEQ and WEPS wind erosion for different arable land management systems in the Argentinean Pampas. Earth Surf. Process. Landf. 33, 1839–1850.
Chadwick, O.A., Derry, L.A., Vitousek, P.M., Huebert, B.J., Hedin, L.O., 1999. Changing sources of nutrients during four million years of ecosystem development. Nature 397, 491–497.
Chappell, A., Sanderman, J., Thomas, M., Read, A., Leslie, C., 2012. The dynamics of soil redistribution and the implications for soil organic carbon accounting in agricultural south-eastern Australia. Glob. Chang. Biol. 18, 2081–2088.
Chappell, A., Webb, N.P., Butler, H.J., Strong, C.L., McTainsh, G.H., Leys, J.F., Viscarra Rossel, R.A., 2013. Soil organic carbon dust emission: an omitted global source of atmospheric CO_2. Glob. Chang. Biol. 19, 3238–3244.
Chen, L., Zhao, H., Han, B., Bai, Z., 2014. Combined use of WEPS and Models-3/CMAQ for simulating wind erosion source emission and its environmental impact. Sci. Total Environ. 466, 762–769.
Conway, T.M., Wolff, E.W., Röthlisberger, R., Mulvaney, R., Elderfield, H.E., 2015. Constraints on soluble aerosol iron flux to the Southern Ocean at the Last Glacial Maximum. Nat. Commun. 6, 7850.
Du, H., Xue, X., Wang, T., 2014. Estimation of the quantity of aeolian saltation sediments blown into the Yellow River from the Ulanbuh Desert, China. J. Arid. Land 6, 205–218.
Duan, H.X., Zhao, J.H., Li, Y.H., 2013. The frequencies, severities, and driving factors of the sand-dust weather processes occurred in Northern China in the Spring of 2011. J. Desert Res. 33, 179–186.
Eger, A., Almond, P.C., Condron, L.M., 2013. Phosphorus fertilization by active dust deposition in a super-humid, temperate environment-Soil phosphorus fractionation and accession processes. Glob. Biogeochem. Cycles 27, 108–118.
Engelstädter, S., Kohfeld, K.E., Tegen, I., Harrison, S.P., 2003. Controls of dust emissions by vegetation and topographic depressions: an evaluation using dust storm frequency data. Geophys. Res. Lett. 30, 1294.
Fécan, F., Marticorena, B., Bergametti, G., 1998. Parametrization of the increase of the aeolian erosion threshold wind friction velocity due to soil moisture for arid and semi-arid areas. Ann. Geophys. 17, 149–157.
Field, J.P., Breshears, D.D., Whicker, J.J., 2009. Toward a more holistic perspective of soil erosion: why aeolian research needs to explicitly consider fluvial processes and interactions. Aeolian Res. 1, 9–17.
Fryrear, D.W., Chen, W.N., Lester, C., 2001. Revised wind erosion equation. Ann. Arid. Zone 40, 265–279.
Fryrear, D.W., Saleh, A., Bilbro, J.D., 1998. A single event wind erosion model. Trans. ASAE 41, 1369–1374.
Gao, H., Yang, S., 2009. A severe drought event in northern China in winter 2008–2009 and the possible influences of La Nina and Tibetan Plateau. J. Geophys. Res. Atmos 114, D24104.
Ginoux, P., Prospero, J.M., Torres, O., Chin, M., 2004. Long-term simulation of global dust distribution with the GOCART model: correlation with North Atlantic Oscillation. Environ. Modell. Softw. 19, 113–128.
Gong, G.L., Liu, J.Y., Shao, Q.Q., Zhai, J., 2014. Sand-fixing function under the change of vegetation coverage in a wind erosion area in northern China. J. Res. Ecol. 5 (2), 105–114.
Gregory, J.M., Wilson, G.R., Singh, U.B., Darwish, M.M., 2004. TEAM: integrated, process-based wind-erosion model. Environ. Modell. Softw. 19, 205–215.
Grigholm, B., Mayewski, P.A., Kang, S., Zhang, Y., Morgenstern, U., Schwikowski, M., Kaspari, S., Aizen, V., Aizen, E., Takeuchi, N., Maasch, K.A., Birkel, S., Handley, M., Sneed, S., 2015. Twentieth century dust lows and the weakening of the westerly winds over the Tibet. Plateau. Geophys. Res. Lett. 42, 2434–2441.
Guo, Z., Zobeck, T.M., Zhang, K., Li, F., 2013. Estimating potential wind erosion of agricultural lands in northern China using the Revised Wind Erosion Equation and geographic information systems. J. Soil Water Conserv. 68, 13–21.
Gutman, G., Ignatov, A., 1998. The derivation of the green vegetation fraction from NOAA/AVHRR data for use in numerical weather prediction models. Int. J. Remote Sens. 19, 1533–1543.
Hoffmann, C., Funk, R., Reiche, M., Li, Y., 2011. Assessment of extreme wind erosion and its impacts in Inner Mongolia, China. Aeolian Res. 3, 343–351.
Horner, T.J., Williams, H.M., Hein, J.R., Saito, M.A., Burton, K.W., Halliday, A.N., Nielsen, S.G., 2015. Persistence of deeply sourced iron in the Pacific Ocean. P. Natl. Acad. Sci. U. S. A. 112, 1292–1297.
Jickells, T.D., An, Z.S., Andersen, K.K., Baker, A.R., Bergametti, G., Brooks, N., Cao, J.J., Boyd, P.W., Duce, R.A., Hunter, K.A., Kawahata, H., Kubilay, N., laRoche, J., Liss, P.S., Mahowald, N., Prospero, J.M., Ridgwell, A.J., Tegen, I., Torres, R., 2005. Global iron connections between desert dust, ocean biogeochemistry, and climate. Science 308, 67–71.
Kurosaki, Y., Mikami, M., 2007. Threshold wind speed for dust emission in east Asia and its seasonal variations. J. Geophys. Res. Atmos. 112, D17202.
Lambert, F., Delmonte, B., Petit, J.R., Bigler, M., Kaufmann, P.R., Hutterli, M.A., Stocker, T.F., Ruth, U., Steffensen, J.P., Maggi, V., 2008. Dust-climate couplings over the past 800,000 years from the EPICA Dome C ice core. Nature 452, 616–619.
Li, F., Zeng, Y., Li, X., Zhao, Q., Wu, B., 2014. Remote sensing based monitoring of interannual variations in vegetation activity in China from 1982 to 2009. Sci. China Earth Sci. 57, 1800–1806.
Li, J., Okin, G.S., Alvarez, L., Epstein, H., 2007. Quantitative effects of vegetation cover on wind erosion and soil nutrient loss in a desert grassland of southern New Mexico, USA. Biogeochemistry 85, 317–332.
Li, Z., 2015. Driving Mechanism for Wind Speed. Study on Climate Change in Southwestern China. Springer Berlin Heidelberg, Berlin, German, pp. 180–188.
Liu, S., Wang, T., 2014. Aeolian processes and landscape change under human disturbances on the Sonid grassland of inner Mongolian Plateau, northern China. Environ. Earth Sci. 71, 2399–2407.
Lu, H., Shao, Y., 2001. Toward quantitative prediction of dust storms: an integrated wind erosion modelling system and its applications. Environ. Modell. Softw. 16, 233–249.
Ma, Z.G., Fu, C.B., 2006. Some evidence of drying trend over northern China from 1951 to 2004. Chin. Sci. Bull. 51, 2,913–2,925.
Mace, K.A., Kubilay, N., Duce, R.A., 2003. Organic nitrogen in rain and aerosol in the eastern Mediterranean atmosphere: an association with atmospheric dust. J. Geophys. Res. Atmos 108, 4320.
Mahowald, N., Ballentine, J.A., Feddema, J., Ramankutty, N., 2007. Global trends in visibility: implications for dust sources. Atmos. Chem. Phys. 7, 3309–3337.
Maman, S., Blumberg, D.G., Tsoar, H., Mamedov, B., Porat, N., 2011. The Central Asian ergs: a study by remote sensing and geographic information systems. Aeolian Res. 3, 353–366.
Mao, R., Ho, C.H., Feng, S., Gong, D.Y., Shao, Y., 2013. The influence of vegetation variation on Northeast Asian dust activity. Asia Pac. J. Atmos. Sci. 49, 87–94.
Mao, R., Ho, C.H., Shao, Y., Gong, D.Y., Kim, J., 2011. Influence of Arctic Oscillation on dust activity over northeast Asia. Atmos. Environ. 45, 326–337.
McTainsh, G.H., Lynch, A.W., Tews, E.K., 1998. Climatic controls upon dust storm occurrence in eastern Australia. J. Arid. Environ. 39, 457–466.
Miller, R.L., Perlwita, J., Tegen, I., 2004. Feedback upon dust emission by dust radiative forcing through the planetary boundary layer. J. Geophys. Res. Atmos. 109, D24209.
Mulitza, S., Heslop, D., Pittauerova, D., Fischer, H.W., Meyer, I., Stuut, J.B., Zabel, M., Mollenhauer, G., Collins, J.A., Kuhnert, H., Schulz, M., 2010. Increase in African dust flux at the onset of commercial agriculture in the Sahel region. Nature 466, 226–228.
Munson, S.M., Belnap, J., Okin, G.S., 2011. Responses of wind erosion to climate-induced vegetation changes on the Colorado Plateau. Proc. Natl. Acad. Sci. U. S. A. 108, 3,854–3,859.
Neff, J.C., Ballantyne, A.P., Farmer, G.L., Mahowald, N.M., Conroy, J.L., Landry, C.C.,

Overpeck, J.T., Painter, T.H., Lawrence, C.R., Reynolds, R.L., 2008. Increasing eolian dust deposition in the western United States linked to human activity. Nat. Geosci. 1, 189–195.
Okin, G.S., 2008. A new model of wind erosion in the presence of vegetation. J. Geophys. Res. F. Earth Surf. 113, F02S10.
Piao, S., Fang, J., Zhou, L., Guo, Q., Henderson, M., Ji, W., Li, Y., Tao, S., 2003. Interannual variations of monthly and seasonal normalized difference vegetation index (NDVI) in China from 1982 to 1999. J. Geophys. Res. Atmos. 108, 4401.
Piao, S., Mohammat, A., Fang, J., Cai, Q., Feng, J., 2006. NDVI-based increase in growth of temperate grasslands and its responses to climate changes in China. Glob. Environ. Chang. 16, 340–348.
Qian, W., Quan, L., Shi, S., 2002. Variations of the dust storm in China and its climatic control. J. Clim. 15, 1216–1229.
Reiche, M., Funk, R., Zhang, Z., Hoffmann, C., Reiche, J., Wehrhan, M., Li, Y., Sommer, M., 2012. Application of satellite remote sensing for mapping wind erosion risk and dust emission-deposition in Inner Mongolia grassland, China. Grassl. Sci. 58, 8–19.
Reynolds, R., Belnap, J., Reheis, M., Lamothe, P., Luiszer, F., 2001. Aeolian dust in Colorado Plateau soils: nutrient inputs and recent change in source. P. Natl. Acad. Sci. U. S. A. 98, 7123–7127.
Shao, Y., Jung, E., Leslie, L.M., 2002. Numerical prediction of northeast Asian dust storms using an integrated wind erosion modeling system. J. Geophys. Res. Atmos. 107, AAC-21.
Shao, Y., Leslie, L.M., 1997. Wind erosion prediction over the Australian continent. J. Geophys. Res. 102, 30–091.
Shao, Y., Yang, Y., Wang, J., Song, Z., Leslie, L.M., Dong, C., Zhang, Z., Lin, Z., Kanai, Y., Yabuki, S., Chun, Y., 2003. Northeast Asian dust storms: Real-time numerical prediction and validation. J. Geophys. Res. Atmos. 108, AAC-3.
Sokolik, I.N., Toon, O.B., 1996. Direct radiative forcing by anthropogenic airborne mineral aerosols. Nature 381, 681–683.
Sun, J., Zhang, M., Liu, T., 2001. Spatial and temporal characteristics of dust storms in China and its surrounding regions, 1960-1999: Relations to source area and climate. J. Geophys. Res. Atmos. 106, 10,325–10,333.
Tanaka, T., Chiba, M., 2006. A numerical study of the contributions of dust source regions to the global dust budget. Glob. Planet. Chang. 52, 88–104.
Taramelli, A., Pasqui, M., Barbour, J., Kirschbaum, D., Bottai, L., Busillo, C., Calastrini, F., Guarnieri, F., Small, C., 2012. Spatial and temporal dust source variability in northern China identified using advanced remote sensing analysis. Earth Surf. Process. Landf. 38, 793–809.
Tegen, I., Fung, I., 1994. Modeling of mineral dust in the atmosphere: sources, transport, and optical thickness. J. Geophys. Res. Atmos. 99, 22,897–22,914.
Tucker, C.J., Pinzon, J.E., Brown, M.E., Slayback, D.A., Pak, E.W., Mahoney, R., Vermote, E.F., El Saleous, N., 2005. An extended AVHRR 8-km NDVI dataset compatible with MODIS and SPOT vegetation NDVI data. Int. J. Remote Sens. 26, 4485–4498.
Wang, A., Lettenmaier, D.P., Sheffield, J., 2011. Soil moisture drought in China, 1950-2006. J. Clim. 24, 3257–3271.
Wang, N., 2005. Decrease trend of dust event frequency over the past 200 years recorded in the Malan ice core from the northern Tibetan Plateau. Chin. Sci. Bull. 50, 2866–2871.
Wang, T., 2014. Aeolian desertification and its control in Northern China. Intern. Soil Water Conserv. Res. 2, 34–41.
Wang, T., Wu, W., Xue, X., Han, Z., Zhang, W., Sun, Q., 2004. Spatial-temporal changes of sandy desertified land during last 5 decades in northern China. ACTA Geogr. Sin. Chin. Ed. 59, 203–212.
Wang, Z., Panmao, Z., Zhang, H., 2003. Variation of drought over northern China during 1950–2000. J. Geogr. Sci. 13, 480–487.
Webb, N.P., McGowan, H.A., Phinn, S.R., Leys, J.F., McTainsh, G.H., 2009. A model to predict land susceptibility to wind erosion in western Queensland, Australia. Environ. Modell. Softw. 24, 214–227.
Xu, D., Li, C., Song, X., Ren, H., 2014. The dynamics of desertification in the farming-pastoral region of North China over the past 10 years and their relationship to climate change and human activity. Catena 123, 11–22.
Yu, M., Li, Q., Hayes, M.J., Svoboda, M.D., Heim, R.R., 2014. Are droughts becoming more frequent or severe in China based on the standardized precipitation evapotranspiration index: 1951–2010? Int. J. Climatol. 34, 545–558.
Zender, C.S., Kwon, E.Y., 2005. Regional contrasts in dust emission responses to climate. J. Geophys. Res. Atmos. 110, D13201.
Zhou, Z.J., Zhang, G.C., Ai, W.X., Zhang, H.Z., Niu, R.Y., 2006. Time series of spring dust emission and its correlative climatic factors in northern China. J. Desert Res. 26, 935–941.
Zobeck, T.M., Parker, N.C., Haskell, S., Guoding, K., 2000. Scaling up from field to region for wind erosion prediction using a field-scale wind erosion model and GIS. Agri. Ecosys. Environ. 82, 247–259.